THE AMERICAN SOCIETY OF MECHANICAL ENGINEERS
345 E. 47 St., New York, N.Y. 10017

89-GT-12

Study of Various Factors Affecting Secondary Loss Vortices Downstream a Straight Turbine Cascade

A. MOBARAK, Professor
M. G. KHALAFALLAH, Professor
Cairo University, Egypt
H. A. HEIKAL, Professor
Helwan University, Egypt
A. M. OSMAN, Lecturer
Zagazig University, Egypt

ABSTRACT

An experimental investigation is carried out to study the effect of inlet boundary layer thickness, aspect ratio and exit Mach number on the energy loss and on the behaviour of secondary vortices downstream of a straight turbine cascade of blades having 82° turning angle.

Some correlations were deduced which predict, the cascade efficiency and the gross secondary loss coefficient as function of the downstream distance.

NOMENCLATURE

AR=h/c	Blade aspect ratio.
b	Axial chord length.
C	Absolute velocity
c	Blade chord length.
H	Shape factor.
h	Static enthalpy or blade height.
h_o	Stagnation enthalpy or reference blade height equals to 64 mm.
k	Isentropic index.
ℓ	Distance from trailing edge in streamwise direction.
M	Mach number.
m	Index in power law of the inlet boundary layer-velocity profile expression.
P	Pressure.
R_a	Arithmetic average height of surface roughness
r_o	Leading edge radius.
S	Blade pitch
t	Maximum thickness.
t_e	Trailing edge thickness.
x	Axial coordinate along the cascade axis.
Y	Stagnation pressure loss coefficient.
y	Pitch-wise coordinate.
Z	Spanwise coordinate measured from the cascade lower endwall
β'	Blade angle measured from tangential direction.
δ	Boundary layer thickness.
δ^*	Displacement thickness.
ϵ	Blade turning angle.
ξ	Enthalpy loss coefficient based on isentropic heat drop.
ξ'	Enthalpy loss coefficient based on actual heat drop.
ξ_{SG}	Gross secondary loss coefficient.
η	Cascade efficiency.
θ	Momentum thickness.

Subscripts

o	Stagnation condition
1	Inlet to the cascade.
2	Outlet from the cascade.
ms	Midspan values
s	Isentropic

Superscripts

-	Pitch-averaged values
=	Pitch and span averaged values.

INTRODUCTION

Use of small power turbines is characterised by the small dimensions of the stage as a result of the limited mass flow rate. This is greatly reflected upon the turbine performance as it is necessary to use low aspect ratio blades and/or partial admission. In both cases, it is very important to specify the optimum configuration that makes the total energy loss as low as possible.

In turbines of low aspect ratio, secondary losses form a significant part of total losses and their reduction would offer a substantial potential to improve efficiency.

Presented at the Gas Turbine and Aeroengine Congress and Exposition—June 4–8, 1989—Toronto, Ontario, Canada

At the end walls, the inlet boundary layer separates near the leading edge and forms a leading vortex with one leg in the suction surface of the blade and the other leg crossing the passage to meet the suction surface of the adjacent blade. The pressure gradient between pressure and suction surface also leads to flow from the pressure to suction surface in the boundary layer on the wall. This flow reinforces the pressure side leg of the leading edge vortex and both with the entrained fluid from the main stream flow in the cascade passage form the passage vortex (Langston, 1980). Due to this flow on the wall, low energy material accumulates near the wall on the suction surface. Behind the trailing edges, the passage vortex comprises the low energy material which has accumulated near the suction surface (Binder and Romey , 1983).

In the last ten years, detailed studies of flow in turbine cascade have been carried out by various investigators. For example , Came (1973) and Chen and Dixon (1985) show that the gross secondary flow and mixing process downstream of the cascade are affected by the inlet boundary layer thickness. Langston et al. (1977) show that about one-third to one-half of the losses occurring downstream presumably due to mixing out of a nonuniform flow at the blade exit.

In the present paper, experimental investigation is directed towards the study of the effect of inlet boundary layer thickness, aspect ratio and exit Mach number on the local values of energy loss coefficient and on the behaviour of secondary vortices downstream the turbine cascade of blades.

The aspect ratio was changed by changing the blade height and keeping the chord constant.

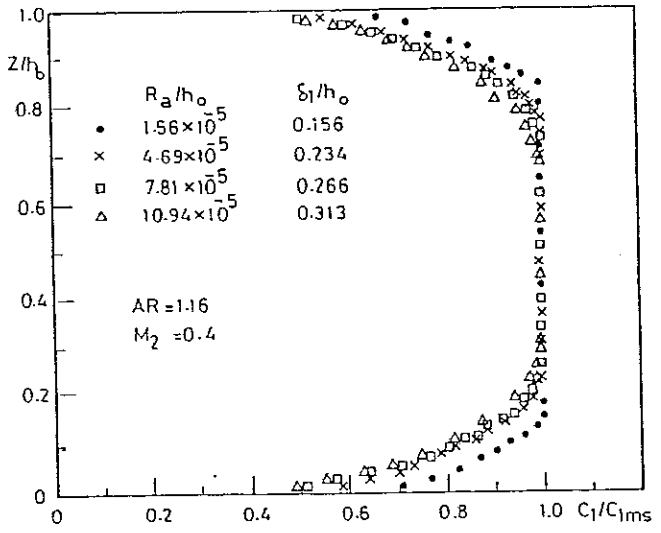

Fig. 1 Spanwise distribution of the inlet boundary layer velocity profiles.

EXPERIMENTAL FACILITY

The cascade, test facilities, test evaluation, instrumentation and measurements are described in detail in Mobarak et al.,(1988). Only a few of the main features of the test facilities will be given here.

The main geometric details of the tested cascade of blades are given in Table 1. The number of blades for the tested cascade are seven in order to have a pitch to chord ratio of 0.61 which is the optimum value corresponding to the tested blade profile (Abdel Hafiz, 1982).

Table 1: Geometry of the turbine cascade.

Blade chord length, c(mm)	55
Blade axial chord, b, (mm)	43
Leading edge radius, r_o(mm)	3.5
Blade height, h_o (mm)	64
Blade aspect ratio, h/c	1.16
Pitch/chord ratio, S/c	0.61
Maximum thickness to chord ratio, t/c	0.264
Trailing edge thickness to pitch ratio t_e/S	0.0147
Inlet blade angle, β'_1	83°
Outlet blade angle, β'_2	14°
Blade turnining angle, ε	83°

$\varepsilon = 180 - (\beta'_1 + \beta'_2)$

The inlet boundary layer was measured with a boundary layer probe of 0.5 mm diameter. The inlet boundary layer was changed by sticking sand papers on upper and lower endwalls before, through and after the cascade in order to simulate the real case when the roughness of these surfaces may be changed. This is because in real situation all the surface will be roughened and not only that part before the cascade. Figure 1 shows the shape of inlet velocity and boundary layer profiles for different values of relative arithmetic average heights (R_a/h_o). The velocity profile can be described by the relation:

$$\frac{C_1}{C_{1ms}} = (Z/\delta_1)^m \qquad (1)$$

The values of boundary layer parameters may be obtained as given in Table 2.

Table 2: Inlet boundary layer properties for AR = 1.16 and M_2 = 0.4

R_a/h_o	δ_1 (mm)	m	δ_1/h_o	δ_1^* (mm)	θ_1 (mm)	H_1	δ_1^*/c
1.56×10^{-5}	10	0.215	0.156	1.77	1.237	1.43	0.042
4.96×10^{-5}	15	0.220	0.234	2.70	1.878	1.44	0.049
7.81×10^{-5}	17	0.216	0.266	3.02	2.109	1.43	0.055
10.9×10^{-5}	20	0.210	0.313	3.47	2.440	1.42	0.063

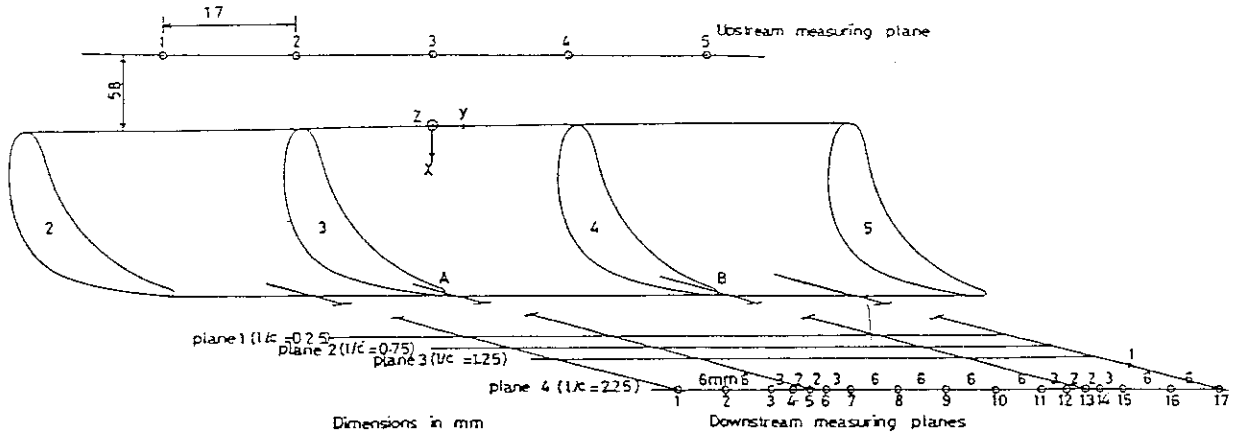

Fig. 2 Inlet and exit measuring stations as distributed in pitchwise direction.

The inlet turbulence intensity at the central passage was measured using a hot wire anemometer probe for different values of the tested parameters and it was found to vary within 2-3%.

To check the periodicity of flow through the cascade, measurements were carried out at cascade exit and it was found that the similarity of velocity profiles exists.

Measurements of flow parameters were performed at four different planes downstream of the cascade by using a five-hole probe of 3 mm diameter. The distances of the measuring planes from trailing edge were measured in the streamwise direction and these planes are located at ℓ/c = 0.25, 0.75, 1.25 and 2.25 , where "ℓ" is the streamwise distance, Fig.2. These planes correspond to an axial distance ratios x/c = 0.06, 0.18, 0.30 and 0.54.

The slope angles of flow were measured at exit plane and it was found to be equal zero at midspan for all tested parameters.

Tests were conducted at an air speed such that the blade chord Reynolds number was varied from 2.2×10^5 to 5.5×10^5 based on the average outlet velocity, which is relatively high. Thus, the effect of Reynolds number on loss coefficient can be neglected, (Kacker and Okapuu, 1981). Local values of total energy loss coefficient corresponding to each exit measuring station was calculated using the relation:

$$\xi = \frac{h_2 - h_{2s}}{h_{o2} - h_{2s}} = \frac{\left(P_{o1}/P_{o2}\right)^{\frac{k-1}{k}} - 1}{\left(P_{o1}/P_2\right)^{\frac{k-1}{k}} - 1} \qquad (2)$$

The pitch-averaged and passage-averaged energy loss coefficients were calculated on mass-averaged basis.

RESULTS AND DISCUSSION

The experimental results are given at the optimum incidence. The incidence angle was changed for all tested values of inlet boundary layer thickness, aspect ratio and exit Mach number. It was found that the optimum incidence is zero degree.

The local loss coefficient maps at AR = 1.16, $\delta 1/h_o$ = 0.156 and M_2 = 0.4 are given in figures 3-6 for different values of the distance downstream ℓ/c = 0.25, 0.75, 1.25 , and 2.25 respectively.

The results shown in Fig.3 at ℓ/c = 0.25 indicate that the loss characteristics at the trailing edges are similar and the high loss zones appear near the endwalls. It is clear from this figure that the regions of low energy (which are characterised by two peaks of energy loss or cores of loss) lie near the suction surface and the endwalls. These two regions of high loss lie at 12.5% and 87.5% of the blade span from the lower end wall. The two cores of loss are not caused by the wake, they are the result of secondary flows within the blade passage. The development of such loss regions is described in the works of Marchal and Sieverding (1977), Langston(1980) and Sharma and Butler (1986).

Figure 3 is a typical one for the total energy loss contours at the trailing edge of straight nozzle blade cascades as obtained by many investigators.

Moustapha et al.(1985) tested planar and annular cascades having the same aspect ratio of 0.88 and turning angle of 128.5°. Results for the planar cascade show that there are two high loss cores close and parallel to the projection of the blade suction surface at 0.32 and 0.65 of the blade span. For the annular cascade, a large high loss core is visible at the middle of the blade passage between 0.48 and 0.77 span. He attributed it to the

varying pitch to chord ratio, the orientation of the blades in the annulus, and the radial pressure gradients occurring in the annular cascade. These factors have a combined effect on the merging of the two passage vortices and the radial position of the resulting high loss core.

Ye Da-Jun and Zhou Li-Wei (1985) tested a rectilinear cascade of 1.047 aspect ratio and 70° turning angle. They found that the positions of the loss cores lie at 0.2 span from the neighbouring end wall.

From the above comparison, it is clear that the aspect ratio and turning angle of the rectilinear cascade affect on positions of the secondary flow patterns.

The total energy loss coefficient contour plots for ℓ/c = 0.75 and 1.25 are shown in Figs.4 and 5 respectively. Both mixing of the wake and pitchwise flow of the low energy material towards the pressure side are clear in these figures. The wake width gets wider and the loss values within the wake decrease due to fluid mixing between the low energy fluid in the wake and the high energy fluid outside it. Also, the loss regions near the end walls are more extended but their intensity is reduced as a result of mixing. The effect of deviation and pressure difference on the blade surfaces is to displace the loss cores towards the pressure side of the adjacent blade as it flows downstream

At ℓ/c = 2.25, Fig.6, the discrete regions of high losses have disappeared and the wake itself is scarcely visible because of mixing. Due to the nearly uniform stream, the iso-loss lines become horizontal and the losses are low except at regions close to end walls.

It is clear from Figs 3-6 that the spanwise positions of the loss cores are approximately constant with distance downstream.

Therefore, it can be concluded that the effect of mixing downstream of a straight cascade is to decrease the intensity of secondary vortices.

Figures 3 and 7-9 illustrate the total energy loss contours at ℓ/c = 0.25 for the case of AR = 1.16, M_2 = 0.4 and for four different values of inlet boundary layer thickness to span ratios (δ_1/h_o) namely 0.156, 0.234 0.266 and 0.313 respectively. It is observed that large areas of the flow are virtually loss free while there is a significant loss increase within the blade wakes and in the regions close to the end walls.

The total energy loss distribution shows clearly the expected increase in loss at the end walls due to the effect of boundary layer loss and the extension of it towards the midspan in the wake region due to secondary flows.

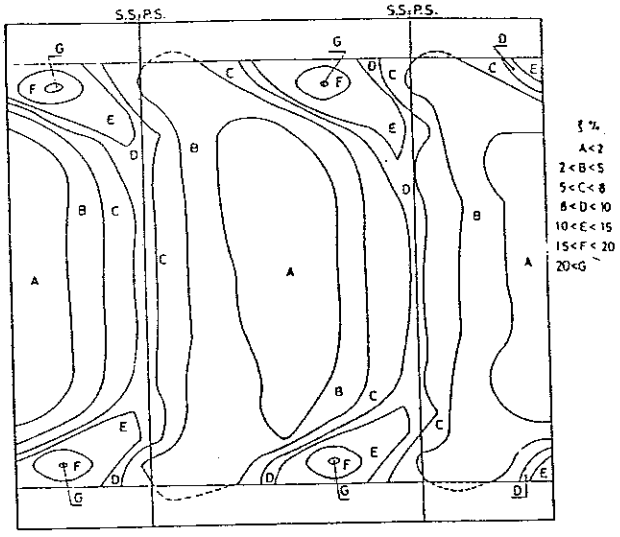

Fig. 4 Total energy loss contours at ℓ/c=0.75 for δ_1/h_o = 0.156, AR = 1.16 and M_2=0.4

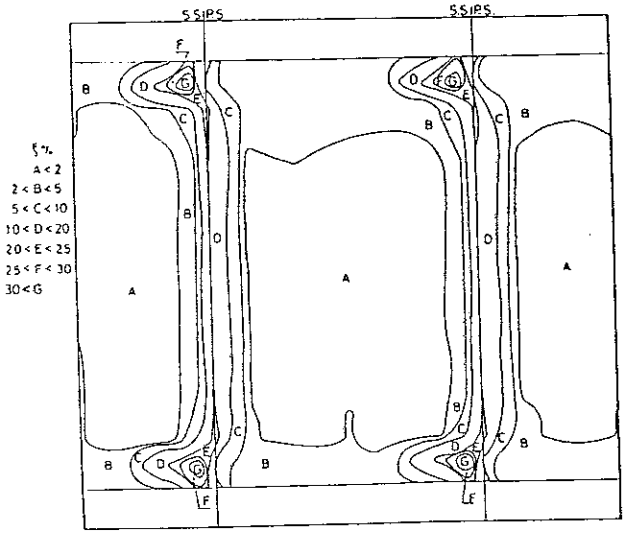

Fig. 3 Total energy contours at ℓ/c = 0.25 for δ_1/h_o = 0.156, AR = 1.16 and M_2 = 0.4.

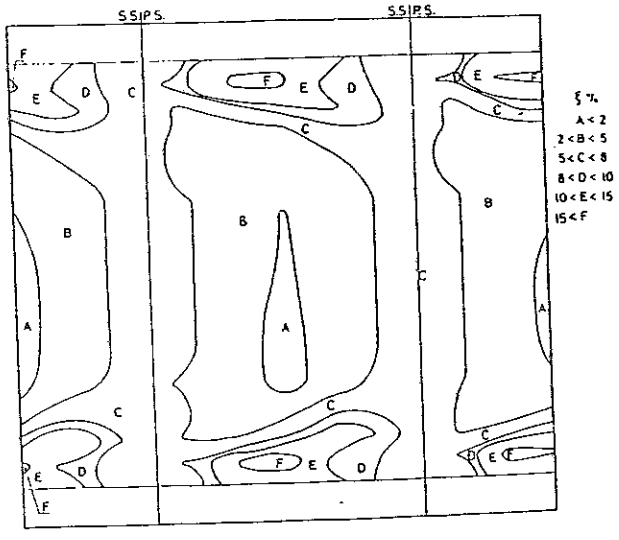

Fig. 5 Total energy loss contours at ℓ/c=1.25 for δ_1/h_o =0.156, AR=1.16 and M_2=0.4

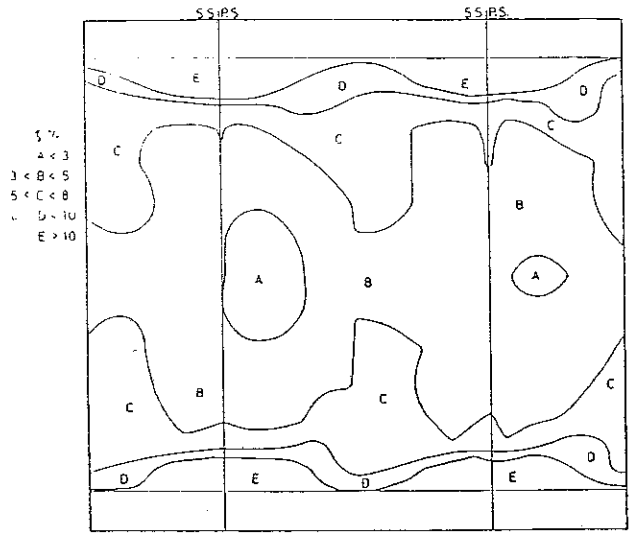

Fig. 6 Total energy contours at $\ell/c=2.25$ for $\delta_1/h_o=0.156$, AR=1.16 and $M_2=0.4$

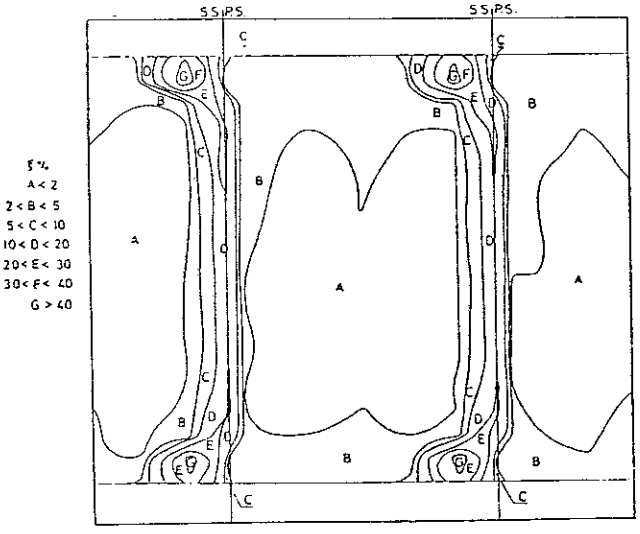

Fig. 7 Total energy contours at $\ell/c = 0.25$ for $\delta_1/h_o=0.234$, AR=1.16 and $M_2=0.4$

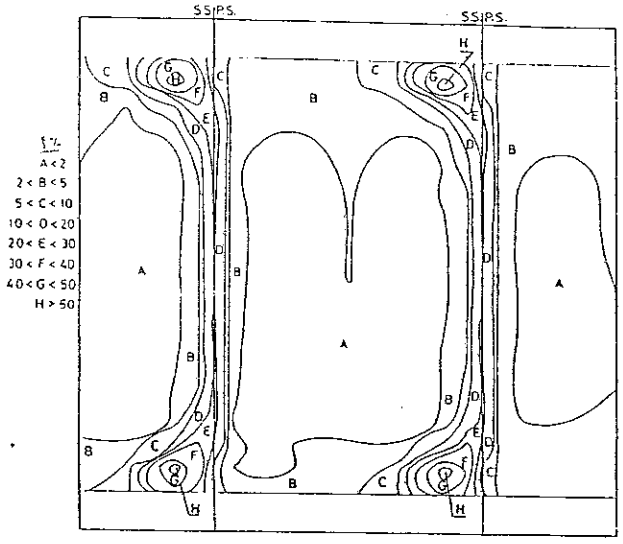

Fig. 8 Total energy contours at $\ell/c=0.25$ for $\delta_1/h_o=0.266$, AR=1.16 and $M_2=0.4$

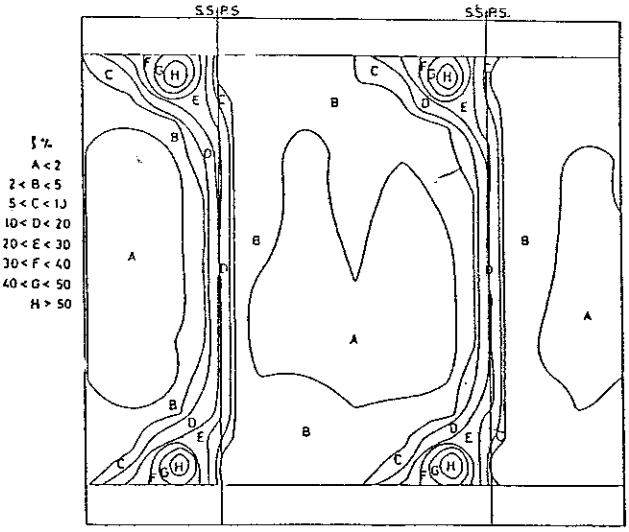

Fig. 9 Total energy contours at $\ell/c = 0.25$ for $\delta_1/h_o = 0.313$, AR=1.16 and $M_2=0.4$

The energy loss peaks are typical of such measurements and correspond to the secondary vortices. The spanwise positions of centre of loss cores are independent of δ_1/h_o and lie at about 12.5% of the blade span from the neighbouring end wall.

Therefore from the presented results, it is clear that the effect of inlet boundary layer thickness on flow picture behind the cascade is more pronounced near the walls with an increased loss in the vortices regions and tendency to move towards the midspan.

Figures 3 and 10-12 illustrate the contours of total energy loss coefficient at $\ell/c = 0.25$ for the four investigated values of aspect ratio. The most striking aspect of the loss contour plots is the loss core region situated on the suction side of the wake center line. Reducing blade aspect ratio from 1.16 to 0.8, the two cores of loss were shifted from a spanwise location of 12.5% to about 20% from the neighbouring wall. With further reduction of AR to 0.5, Fig.11, the two cores of loss approach each other which increases energy loss at blade midspan. The spanwise location of the loss cores lie at 25.5% of the blade height from the end walls.

As it is mentioned in Moustapha et al., (1985), Woods experimental results indicated that the loss peak was shifted from a spanwise location of 15% to about 24% as the aspect ratio was reduced from 1.036 to 0.592.

For the lowest value of tested aspect ratio (AR = 0.25) the two cores of loss

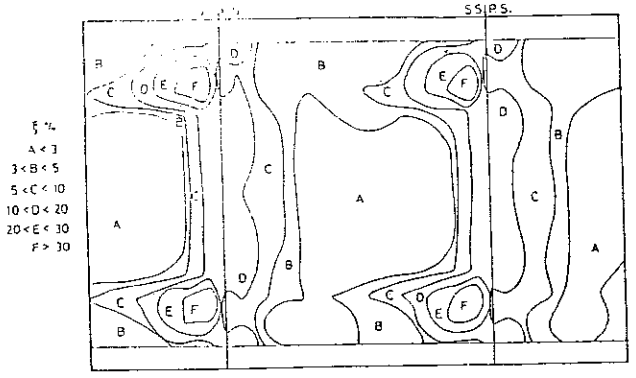

Fig. 10 Total energy contours at ℓ/c = 0.25 for δ_1/h_o= 0.156, AR=0.8 and M_2=0.4.

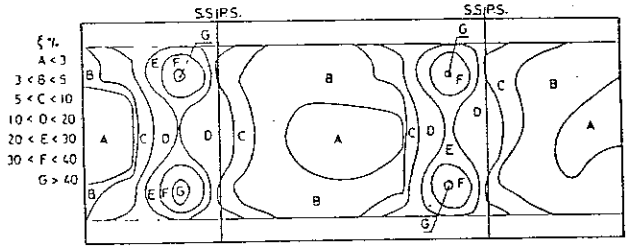

Fig. 11 Total energy contours at ℓ/c = 0.25 for δ_1/h_o=0.156, AR =0.5 and M_2=0.4

combine together to form a single strong loss core at the midspan as shown in Fig.12. Moreover, this single core occupies a great portion of the exit area.

Figures 13 and 14 illustrate the total energy loss contours at the exit plane (ℓ/c = 0.25) for two values of M_2 which are 0.2 and 0.5 respectively. It is worthy to mention that the effect of increasing Mach number is to decrease local values of energy loss coefficient.This is a well known behaviour for subsonic flow as the increase of Mach number improves the profile loss and helps in displacing the cores of secondary vortices towards the blade suction surface. This, in turn, help in increasing the potential core at passage exit and improves the cascade performance. The shape of the 20% iso-loss line at the end wall for M_2 = 0.2 (Fig.13) indicates the presence of corner losses. With increasing Mach number, this phenomenon tends to disappear.

The Gross Secondary Loss

For high aspect ratio blades, the gross secondary losses are determined by subtracting the measured midspan (profile) pitchwise-averaged loss coefficient from the passage - averaged loss coefficient. For low aspect ratio blades used in the present tests, the differentiation between the profile and the secondary loss is difficult due to the merging of vortices (Moustapha et al.,1985). Therefore the gross secondary loss is evaluated for AR= 1.16 only.

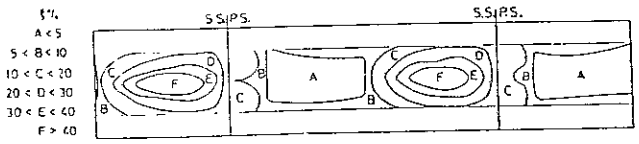

Fig. 12 Total energy contours at ℓ/c=0.25 for δ_1/h_o =0.156, AR=0.25 and M_2=0.4

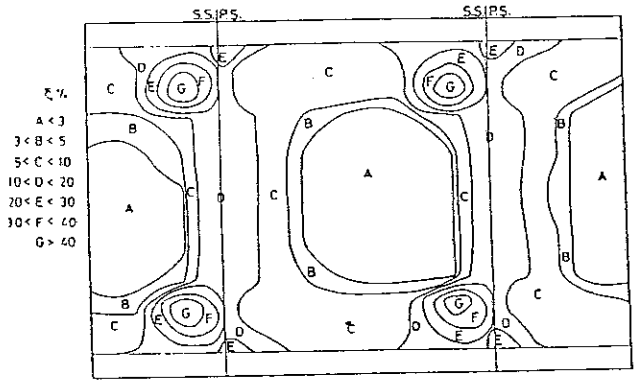

Fig. 13 Total energy contours at ℓ/c=0.25 for δ_1/h_o=0.156, AR=0.8 and M_2=0.2

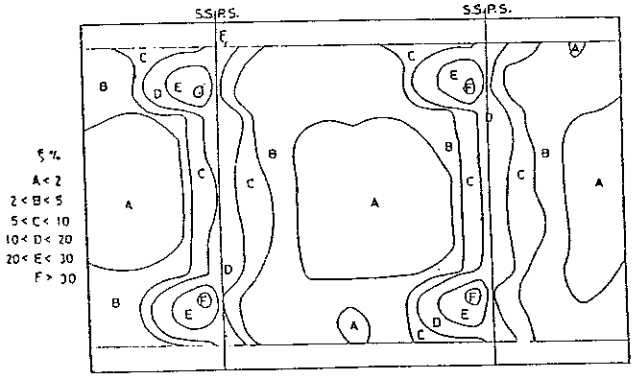

Fig. 14 Total energy contours at ℓ/c =0.25 for δ_1/h_o=0.156, AR=0.8 and M_2=0.5

Figure 15 shows the variation of the gross secondary loss coefficient with the downstream distance to chord ratio (ℓ/c) for different values of relative upstream boundary layer thickness (or boundary layer displacement thickness to chord ratio δ_1^*/c) at AR = 1.16 and M_2 = 0.4.

It is clear from this figure that the gross secondary loss coefficient increases with the increase of ℓ/c and with the increase of the value δ_1/h_o (or δ_1^*/c). Also it is evident that the loss coefficient increase rapidly with ℓ/c for higher values of δ_1/h_o (or δ_1^*/c). This behaviour may be attributed to the redistribution and the growth of additional loss due to the skin friction on the endwalls. This additional loss may be significant for high values of δ_1/h_o because of the effect of large velocity gradients produced near the endwalls.

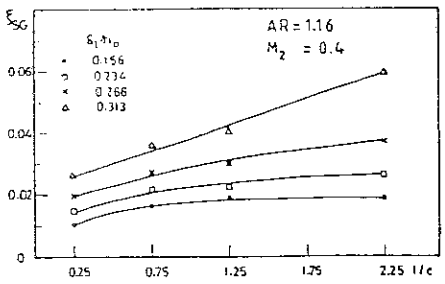

Fig. 15 Variation of gross secondary loss with ℓ/c.

Sieverding and Wilputte (1981), found from tests on a linear cascade of aspect ratio near unity that the secondary loss coefficient does not vary greatly in a range of M_2 from 0.1 to 0.6. Therefore, the effect of Mach number on the gross secondary loss is not included in the following correlations.

Simple correlations of the gross secondary loss coefficient with the distance downstream and with the inlet boundary layer displacement thickness can be derived from Fig. 15 immediately.

The relation between the gross secondary loss coefficient (ξ_{SGO}) at $\delta^*_{1o}/c = 0.032$ and ℓ/c given by:

$$\xi_{SGO} = 0.0183 - \frac{2.352 \times 10^{-4}}{(\ell/c)^{2.5}} \qquad (3)$$

The variation of loss coefficient (ξ_{SG}) with δ^*_1/c, away from ξ_{SGO} at a particular thickness ratio δ^*_{1o}/c, can be given in the form,

$$\xi_{SG} = \xi_{SGO} + E_1\left(\frac{\delta^*_1 - \delta^*_{1o}}{c}\right)^{E_2} \qquad (4)$$

where E_1 and E_2 are constants each of them depends on the distance downstream of the trailing edge,

$$E_1 = 3.157 + 69.6\ (\ell/c)^{2.04} \qquad (5)$$

$$E_2 = 3.506 - \frac{1.153}{(\ell/c)^{0.3}} \qquad (6)$$

Correlation (4) accurately represents the experimental results within $\pm$10% deviations as shown in Fig.16.

Figure 17 shows the variation of the gross secondary loss coefficient with the relative upstream boundary layer displacement thickness for the present test results and other correlations which were deduced by other investigators. Correlations of Dunham and Came(1970), Dunham (1970), Came (1973) and Chen and Dixon (1985) are processed to convert the pressure loss coefficient Y_{SG} to ξ_{SG} for comparison. To convert Y_{SG} to ξ_{SG}, the relations obtained by Horlock (1966) can be used.

$$\xi' = Y/(1+k(M_2^2/2)) \qquad (7)$$

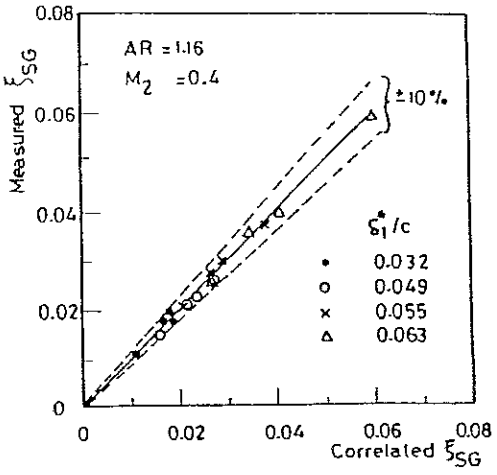

Fig. 16 Correlated ξ_{SG} shows good agreement with measured ξ_{SG}.

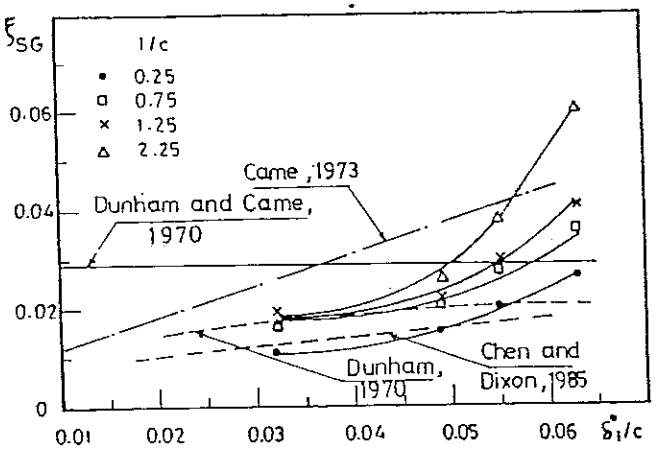

Fig. 17 Variation of gross secondary loss coefficient with inlet displacement thickness.

$$\xi = \xi' / (1 + \xi') \qquad (8)$$

Came (1973) obtained his correlation from data measured at $\ell/c = 1.35$ and Chen's correlation is drawn in Fig. 17 at $\ell/c = 1.35$ while the positions, at which the other two correlations were deduced, are not given.

The present correlation shows a rising trend with increasing the upstream displacement thickness while the correlations deduced by Came (1973), Chen and Dixon (1985) and Dunham (1970) show a constant rate of increase with δ^*_1/c. In contrast, correlation of Dunham and Came (1970) is independent of δ^*_1/c.

The present results show increasing rate of gross secondary loss with δ^*_1/c which may be attributed to the effect of blade shape and regime of operation.

However, it is clear from Fig.17 that the present correlation, at $\ell/c = 1.25$ or the expected at $\ell/c = 1.35$, lies in between Came's and Chen's correlations at $\ell/c = 1.35$.

Tests results are presented in another form in Fig.18 where cascade efficiency ($\eta = 1 - \bar{\zeta}$) is plotted against the reciprocal of AR for different values of ℓ/c at $M_2 = 0.4$ and $\delta_1/h_o = 0.156$.

It is evident that a straight line relationship can be expressed for AR lower than 1.16 (or approximately one) in the form:

$$\eta = E_3 - \frac{E_4}{AR} \qquad \text{for } AR < 1.16 \qquad (9)$$

where E_1 and E_2 are constants that depend on ℓ/c, geometric and aerodynamic parameters of the tested cascade. The term E_3 represents the blade efficiency (or profile efficiency) for AR tends to infinity and given as function of M_2 and ℓ/c, (Osman, 1987).

$$E_3 = 0.9155 + 0.07\, M_2^2 + \frac{0.024}{(\ell/c)^{0.32}} \qquad (10)$$

The values of E_4 which is the slope of the straight line relation η - 1/AR, can be given by, (Osman, 1987).

$$E_4 = 0.0374 - \frac{5.125 \times 10^{-3}}{(\ell/c)^{0.7}} \qquad (11)$$

For the tested cascade of blades, the efficiency at AR = 1.16 is approximately equal to the value of the efficiency corresponding to relatively high aspect ratio blades 1/AR≅0 where secondary losses are neglected and profiles losses exist only.

It is clear from Fig.19 that the correlation (9) gives good agreement with the experimental results within ± 1.2% deviations.

Relations similar to relation (9) were obtained by Ohlsson (1964) for blades of a true tubbine stage having aspect ratio in the range 0.7 - 0.07 and Mobarak et al.(1985) for a straight turbine blades having AR 0.654 - 0.145 at $\ell/c = 0.4$.

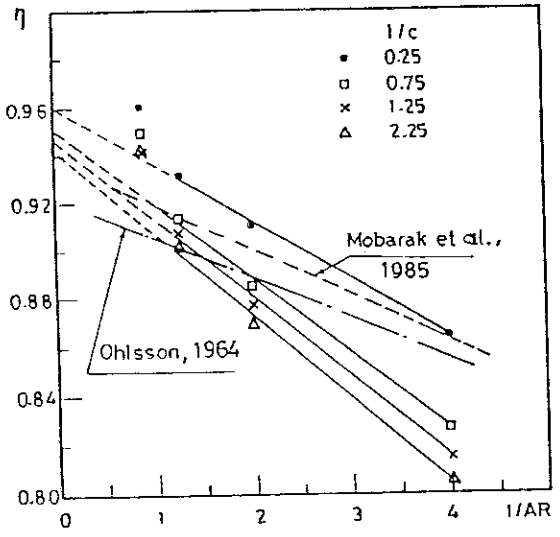

Fig. 18 Cascade efficiency versus 1/AR at $M_2 = 0.4$

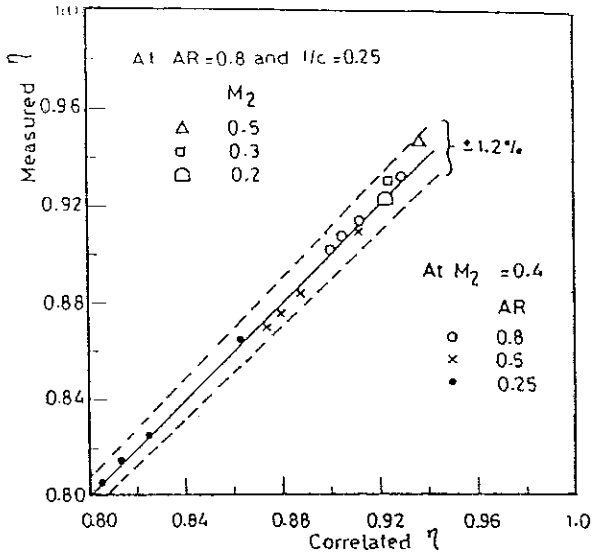

Fig. 19 Correlated efficiency shows good agreement with the present data at $\delta_1/h_o = 0.156$.

It is clear from Fig.18 that Mobarak's and Ohlsson relations give good agreement with the present correlation.

CONCLUSIONS

From the previous results and discussion the following conclusions can be drawn:

1- The analysis of measured energy loss contours show that the spanwise positions of the centres of loss cores are independent of the downstream distance, inlet boundary layer thickness and Mach number. Increasing inlet boundary layer thickness, increases the spanwise extent of the zone behind the cascade in which the secondary loss vortex dominates and in turn the gross secondary loss increases (correlation 4).

2- Reducing blade aspect ratio, the two cores of loss were shifted towards the midspan and combine together at the lower value of aspect ratios (AR = 0.25) to form a single strong loss core. The results show a decreasing rate of the cascade efficiency with reducing aspect ratio due to the contraction of the low loss core of the flow and the increase of endwall effects. It has been found that a straight line relationship could be obtained in the range of AR from 0.8 to 0.25 to relate cascade efficiency and the inverse of AR for different downstream distances. This relation is similar to relations suggested by other investigators at trailing edge for other ranges of aspect ratio lower than one. This means that a generalized relationship can be formulated to cover all values and ranges of aspect ratio lower than one.

REFERENCES

Abdel Hafiz, A.,1982, "Investigation of Flow in Axial Turbines", Ph.D. Thesis, Cairo University.

Binder, A. and Romey, R.,1983,"Secondary Flow Effects and Mixing of the Wake Behind a Turbine Stator", Transactions of the ASME, Journal of Engineering for Power,Vol.105,pp.40-46.

Came, P.M.,1973, "Secondary loss Measurements in a Cascade of Turbine Blades", Institute of Mechanical Engineering Conference,Publ. 3, pp.75-83.

Chen, L.D., and Dixon,S.L.,1985,"Growth of Secondary Flow Losses Downstream of a Turbine Blade Cascade", ASME Paper No. 85-GT-64.

Dunham, J., 1970, "A Review of Cascade Data on Secondary Losses in Turbines", J. Mechanical Engineering Science, Vol.,12, pp.48-59.

Dunham, J. and Came, P.M.1970,"Improvements to the Ainley-Mathieson Method of Turbine Performance Prediction", ASME Paper No.70-GT-2.

Horlock, J.H., 1966, "Axial Flow Turbines", Butterworths Publishers, London, Chapter 3

Kacker, S.C., and Okapuu, U.,1981,"A Mean line prediction Method for Axial Flow Turbine Efficiency", ASME Paper No. 81-GT-58.

Langston, L.S.,1980,"Cross Flows in a Turbine Cascade Passage", ASME Journal of Engineering for Power, Vol. 102, pp.866-874.

Langston, L.S., Nice, N.L., and Hooper,R. M. 1977, "Three-Dimensional Flow Within a Turbine Cascade Passage", ASME Journal of Engineering for Power, Vol.99, pp.21-28.

Marchal, Ph., and Sieverding,C.H.,1977, "Secondary Flows Within Turbomachinery Bladings", AGARD Conference Proceedings No. 214 on Secondary Flows in Turbomachines,The Hague The Netherlands.

Mobarak, A., Khalafallah, M.G., Heikal H.A. and Osman, A.M.,1988,"Experimental investigation of Secondary Flow and Mixing Downstream of Straight Turbine Cascades", ASME Paper No. 88-GT-8.

Mobarak, A., Khalafallah, M.G. and Lotayef, M., 1985, "Effect of Aspect Ratio on Energy Loss in Nozzle Blades of Small Power Turbines", International Journal of Turbo and Jet-Engines, Vol. 2 , pp. 299-305.

Moustapha, S.H., Paron,G.J. and Wade,J.H. T., 1985 "Secondary Flow in cascades of Highly Loaded Turbine Blades", ASME Paper No. 85-GT-135.

Ohlsson, G.O., 1964, "Low Aspect Ratio Turbines", Transactions of the ASME, Journal of Engineering for Power, pp. 13-17.

Osman, A.M.,1987,"Investigation of Secondary Flow and Mixing Downstream of Straight Turbine Cascades", Ph.D. Thesis, Cairo Univeristy.

Sharma, O.P., and Butler, T.L.,1986,"Predictions of Endwall Losses and Secondary Flows in Axial Flow Turbine Cascades",ASME Paper No. 86-GT-228.

Sieverding, C.H. and Wilputte,Ph., 1981, "Influence of Mach Number and End Wall Cooling on Secondary Flows in a Straight Nozzle Cascade" ASME, J. of Engineering for Power, Vol. 103, pp. 257-264.

Ye Da-Jun and Zhou Li-Wei, 1985,"Experimental Research of the Secondary Flow in Rectilinear Turbine Cascades", ASME Paper No. 85-IGT-93.

Horlock, J.H., 1966, "Axial Flow Turbines", Butterworths Publishers, London, Chapter 3

Mobarak, A., Khalafallah, M.G., Heikal H.A. and Osman, A.M.,1988,"Experimental investigation of Secondary Flow and Mixing Downstream of Straight Turbine Cascades", ASME Paper No. 88-GT-8.